crystals

MDPI

Article

Effect of an External Electric Field on the Kinetics of Dislocation-Free Growth of Tetragonal Hen Egg White Lysozyme Crystals

Haruhiko Koizumi*, Satoshi Uda, Kozo Fujiwara, Junpei Okada and Jun Nozawa

Institute for Materials Research, Tohoku University, 2-1-1 Katahira, Aoba-ku, Sendai 980-8577, Japan; uda@imr.tohoku.ac.jp (S.U.); kozo@imr.tohoku.ac.jp (K.F.); junpei.t.okada@imr.tohoku.ac.jp (J.O.); nozawa@imr.tohoku.ac.jp (J.N.)

* Correspondence: h_koizumi@imr.tohoku.ac.jp; Tel.: +81-22-215-2103; Fax: +81-22-215-2101

Received: 28 April 2017; Accepted: 9 June 2017; Published: 10 June 2017

Abstract: Dislocation-free tetragonal hen egg white (HEW) lysozyme crystals were grown from a seed crystal in a cell. The rates of tetragonal HEW lysozyme crystal growth normal to the (110) and (101) faces with and without a 1-MHz external electric field were measured. A decrease in the typical growth rates of the crystal measured under an applied field at 1 MHz was observed, although the overall driving force increased. Assuming that the birth and spread mechanism of two-dimensional nucleation occurs, an increase in the effective surface energy of the step ends was realized in the presence of the electric field, which led to an improvement in the crystal quality of the tetragonal HEW lysozyme crystals. This article also discusses the increase in the effective surface energy of the step ends with respect to the change in the entropy of the solid.

Keywords: protein crystals; growth kinetics; electric field; crystal quality

1. Introduction

The three-dimensional (3D) structures of protein molecules are closely related to the proteins found in living organisms. Thus, determination of the 3D structures of protein molecules is important for the advancement of medical science [1]. The 3D structures of protein molecules have typically been determined at synchrotron radiation facilities with high brilliance. A structure determined using data finer than 1.5 Å—which corresponds to the length of a covalent carbon-carbon bond—is needed in order to achieve structure-guided drug design and controlled drug delivery. This means that the collection of many high-order reflections of protein crystals (i.e., high diffraction efficiency — diffractivity) is desired to obtain accurate 3D structures of protein molecules. As such, many researchers have focused on developing a high-brilliance source and/or improving the sensitivity of the detector system [2]. However, useful structural analysis (<1.5 Å) of protein molecules for structure-guided drug design and controlled drug delivery represents only 9% of all protein molecules registered with the Protein Data Bank (PDB; http://www.rcsb.org/pdb/), even using synchrotron radiation facilities with high brilliance, such as SPring-8. This suggests the importance of the growth of high-quality protein crystals that allow the collection of many high-order reflections.

The growth of high-quality single crystals of proteins has been intensively pursued using magnetic fields [3–9], microgravity [10–16], solution flow [17–20], and gel as a growth host media [21–28]. A growth technique mediated by screw dislocations under low supersaturation has also been proposed [29–32]. Techniques in which an electric field is applied to a protein solution have also been actively investigated, with a focus on controlling the nucleation rate [33–49].

We have also previously attempted to control the nucleation process of protein crystals under an applied electrostatic field [50,51] by considering the effect of the field on the nucleation rate from

a thermodynamics perspective. The effect of such a field was attributed to the electrostatic energy added to the chemical potentials of the liquid and solid phases. The electrostatic energy was produced by a large electric field of about 10^4 V/cm associated with an electric double layer (EDL) at the interface between the two phases, which was significantly larger than the actual experimentally-applied field (800 V/cm) [52]. This thermodynamic effect is added not only to the chemical potential, but also to the entropy. In particular, it was thermodynamically determined that the entropy of the solid decreases under an external electric field with a frequency of 1 MHz, and this is expected to result in a decrease in the degree of disorder in the crystal. Therefore, we attempted to improve the crystal quality of tetragonal hen egg white (HEW) lysozyme crystals by applying a 1-MHz external electric field. It was found that the full width at half-maximum (FWHM) of the X-ray diffraction rocking curves for the resulting crystals was lower than that in the absence of an electric field [53]. In addition, for crystals grown in an electric field, the FWHM was almost independent of the order of the diffraction peaks, whereas in the absence of an applied field, the FWHM increased for diffraction peaks with an order higher than 440 reflection [53], which suggests an improvement in local crystal quality. It was also found that the crystal homogeneity was improved under an electric field [54]. The improved crystal quality was attributed to a decrease in the misorientation between subgrains in the crystal [55]. The mechanism involved is not yet fully understood, although it may be related to the incorporation of impurities into the growing crystal.

In situ observation is a powerful tool for investigating the kinetics of protein crystal growth. The incorporation of impurities into the growing crystal has a significant effect on the kinetics of crystal growth. Therefore, the behavior of impurities can be understood by observing the change in crystal growth kinetics. If an external electric field has an effect on impurity incorporation, it would therefore also change the crystal growth kinetics. In this article, we reveal the effect of an external electric field on the incorporation of impurities into a growing crystal with respect to the change in crystal growth kinetics.

2. Experimental Procedure

HEW lysozyme was purchased from Wako Pure Chemical Industries, Ltd. (Osaka, Japan). There is typically a large amount of NaCl present in commercial HEW lysozyme; therefore, NaCl was removed from the HEW lysozyme solutions by dialysis. Tetragonal HEW lysozyme crystals grown from seed crystals were used in this work. Seed crystals were first grown by preparing an 80 mg/mL HEW lysozyme solution and a 1.0 M NaCl in 100 mM sodium acetate buffer solution and mixing them in equal volumes. The solutions were passed through a filter with a pore size of 0.20 μm to remove any foreign particulates or large protein aggregates. The resulting solution consisted of 40 mg/mL HEW lysozyme and 0.5 M NaCl in 100 mM sodium acetate buffer at pH 4.5. The seed crystals were grown from this crystallization solution at 21 °C for 1 day via the hanging drop technique. The grown seed crystals were chemically fixed by a modified version of a previously reported method [56,57]. The solution used for chemical cross-linking was a mixture of 2.5 wt % glutaraldehyde and 0.5 M NaCl in 100 mM sodium acetate buffer. The seed crystals were immersed in the cross-linking solution for 15 min at 23 °C. Therefore, no dislocations were introduced from the seed crystal, although it is possible that dislocations could occur during the growth process after two weeks [58]. This means that no dislocations occur during in situ observation, because the observation time is about one day. After cross-linking, the seed crystals were rinsed and reused because they did not dissolve in the undersaturated solution.

Next, a 100 mg/mL solution of HEW lysozyme and a solution of 1.0 M NaCl in 100 mM sodium acetate buffer were prepared and mixed in equal volumes. The resulting solution consisted of 50 mg/mL HEW lysozyme and 0.5 M NaCl in 100 mM sodium acetate buffer at pH 4.5. A tetragonal HEW lysozyme crystal was grown from a cross-linked seed crystal in a growth cell (25 × 25 × 4 mm). Crystal growth was conducted with and without a 1-MHz electrostatic field, and in situ observations were made using a digital microscope. Figure 1 shows a schematic illustration of the electrode arrangement on both sides of the growth cell. As shown in Figure 1, no current flows into HEW lysozyme solutions.

The electrodes were parallel to the ($\bar{1}10$) face of the seed crystal. Observations were made of the (110) face perpendicular to the electric field , in addition to the (101) face inclined by approximately 18° to the field.

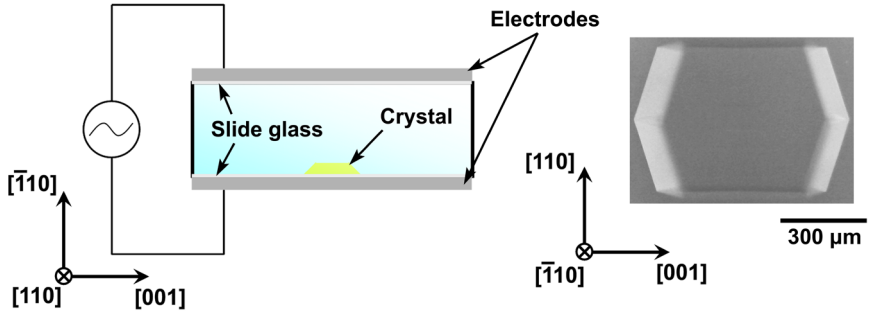

Figure 1. Schematic illustration of the experimental arrangement with electrodes on both sides of the growth cell.

The electric field strength was 1100 V/cm, and indium tin oxide-coated glass slides with a surface resistivity of 8–12 Ω/sq were used as the electrodes. However, in such a situation, it is expected that a large electric field of about 10^4 V/cm would be generated by the EDL at the interface between the solution and the crystal. The growth rate R for the crystals was measured in the presence and absence of the applied field, and the supersaturation σ ($=ln\frac{C}{C_{eq}}$—where C is the concentration of the solution and C_{eq} is the solubility) of the HEW lysozyme solution—was changed by varying the temperature. That is, all growth rates were measured using the same seed crystal at various temperatures. The supersaturation was estimated from the data given in Reference [59].

3. Results

Figure 2 shows the crystal dimensions along the [110] and [001] directions as a function of growth time with and without an external electric field, for a growth temperature at 18 °C.

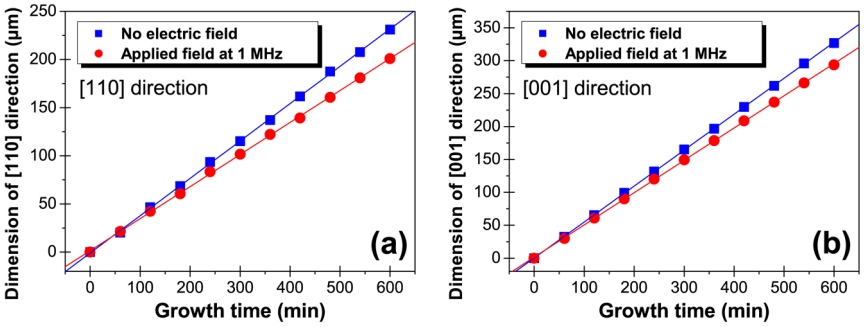

Figure 2. Crystal dimensions along (**a**) [110] and (**b**) [001] directions as function of growth time with and without external electric field, for growth temperature of 18 °C.

It can be seen that for both directions, the dimensions increase linearly with growth time, which indicates that the driving force is unchanged during the measurements. Additionally, the growth rate R, obtained from the slope of the straight lines, is smaller in the case of the applied field. R for the (110) and (101) faces can be calculated from the slope as follows:

$$R_{(110)} = \frac{g_{[110]}}{2}, \quad (1)$$

$$R_{(101)} = \frac{g_{[001]}}{2} cos\theta, \quad (2)$$

where $g_{[110]}$ and $g_{[001]}$ are the slopes obtained for the [110] and [001] directions, respectively, and θ (=25.6°) is the angle between the normal to the (101) surface and the [001] direction. According to Eqations (1) and (2), R for the (110) and (101) faces in an applied field are 9.98 ± 0.06 μm/h and 13.26 ± 0.05 μm/h, respectively, while those in the absence of a field are 11.63 ± 0.07 μm/h and 14.76 ± 0.03 μm/h, respectively. Since the errors involved in these measurements were very small, it can be clearly concluded that the application of an electric field caused a reduction in the growth rate.

Figure 3 shows the dependence of the growth rate for the (110) and (101) faces on the degree of supersaturation. It can be seen that regardless of the supersaturation, the growth rate was always lower in the presence of an electric field. Again, the error bars for these measurements are very small. We have previously demonstrated that the nucleation rate during growth of tetragonal HEW lysozyme crystals increases (i.e., the driving force for nucleation increases) under an external electric field with a frequency of 1 MHz [50]. It might therefore be expected that the growth rate would also increase, in contrast to the results obtained in the present study. This would imply that the growth kinetics are changed under the applied field. We have previously observed that an external electric field does not affect the growth kinetics of YBCO superconductive oxides [60,61]. Therefore, this effect may be unique to protein crystals.

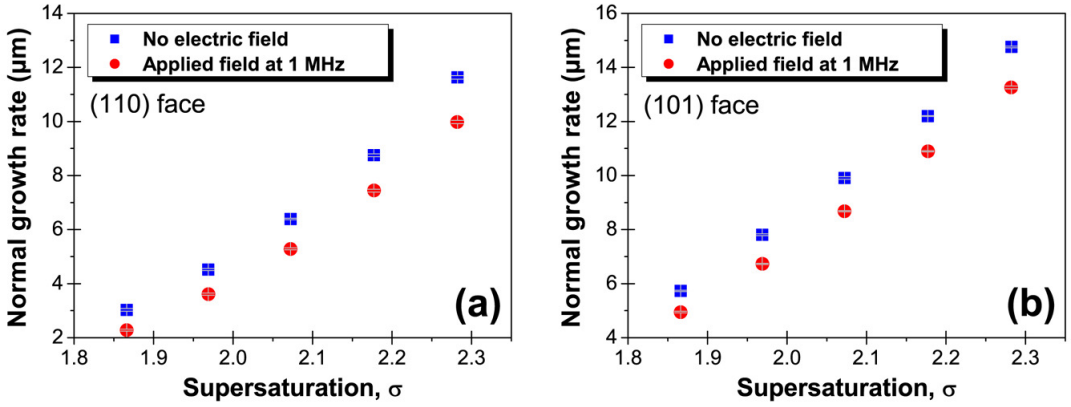

Figure 3. Supersaturation dependence of growth rate for (**a**) (110) and (**b**) (101) faces of tetragonal hen egg white (HEW) lysozyme crystals grown with and without an external electric field.

A dislocation-free crystal cross-linked for 15 min [58] was used in this experiment, so that 2D nucleation and growth of the birth-and-spread type should only occur on the growing faces. Under the range of supersaturations used in this experiment, the formation of multiple nuclei at several points on one growing face (multiple nucleation mode) has been observed for tetragonal HEW lysozyme crystals [62]. The growth rate R using the birth-and-spread model is expressed as [63,64]:

$$R = h(v_{step}^2 J)^{1/3} = h[(\Omega\beta_{step}(C - C_{eq}))^2 J]^{1/3}, \quad (3)$$

where J is the rate of two-dimensional (2D) nucleus formation, v_{step} is the tangential step velocity (which is related to the step kinetic coefficient β_{step} as $v_{step} = \Omega\beta_{step}(C - C_{eq})$ [65]), Ω is the kink volume, and h is the step height.

In the case of the (110) faces of tetragonal HEW lysozyme crystals, an elementary step involves two molecules [66–69]. The rate of 2D nucleus formation J on the (110) face can thus be expressed using a model derived from classical nucleation theory, as follows [62,70]:

$$J = \varpi \Gamma Z exp(-\frac{\pi s \kappa^2}{2k_B^2 T^2 \sigma}), \tag{4}$$

where ϖ is the frequency of attachment of molecules to the critical 2D nucleus, Γ is the Zeldovich factor, Z is the steady-state admolecule surface concentration, s is the area in which one molecule occupies inside the critical 2D nucleus ($s = 1.06 \times 10^{-17}$ m^2) [69], κ is the specific edge free energy, k_B is the Boltzmann constant, and T is the absolute temperature.

On the other hand, in the case of the (101) faces, an elementary step involves one molecule [66–69]; therefore, the rate of 2D nucleus formation J on the (101) face can be expressed according to the classical nucleation theory [62,70]:

$$J = \varpi \Gamma Z exp(-\frac{\pi s \kappa^2}{k_B^2 T^2 \sigma}). \tag{5}$$

Here $s = 7.84 \times 10^{-18}$ m^2 [69].

Substituting Equation (4) into Equation (3) gives the growth rate in the coordinates $ln(R/\sigma^{1/6}(1-e^{-\sigma})^{2/3})$ versus $1/\sigma T^2$ on the (110) face as follows:

$$ln(\frac{R_{(110)}}{\sigma^{1/6}(1-e^{-\sigma})^{2/3}}) = A - \frac{\pi \Omega \alpha^2 h}{6k_B^2}\frac{1}{\sigma T^2}, \tag{6}$$

where α is the effective surface free energy of the step end ($\alpha = \kappa/h$). Here, the step height on the (110) face is taken to be 5.6 nm [62].

In contrast, substituting Equation (5) into Equation (3) gives the growth rate in the coordinates $ln(R/\sigma^{1/6}(1-e^{-\sigma})^{2/3})$ versus $1/\sigma T^2$ on the (101) face as follows:

$$ln(\frac{R_{(101)}}{\sigma^{1/6}(1-e^{-\sigma})^{2/3}}) = A - \frac{\pi \Omega \alpha^2 h}{3k_B^2}\frac{1}{\sigma T^2}. \tag{7}$$

Here, the step height of the (101) face is taken to be 3.4 nm [62].

Figure 4 shows the dependence of the growth rate R with and without an external electric field on $1/(\sigma T^2)$. The effective surface free energy for the step end, α, for the (110) and (101) faces can be estimated using Equations (6) and (7), respectively. Based on the straight line fit to the data in Figure 4a, α with and without an external electric field was estimated to be 1.249 mJ/m^2 and 1.189 mJ/m^2, respectively, for the (110) face. Table 1 shows the effective surface energy for the step end for the (110) and (101) faces with and without an external electric field.

Table 1. Effective surface energy for the step end α for the (110) and (101) faces of tetragonal HEW lysozyme crystals grown with and without an external electric field.

	Surface Energy, α (mJ/m^2)	
	(110) Face	**(101) Face**
No electric field	1.189 ± 0.009	1.329 ± 0.037
Applied field at 1 MHz	1.249 ± 0.023	1.364 ± 0.027

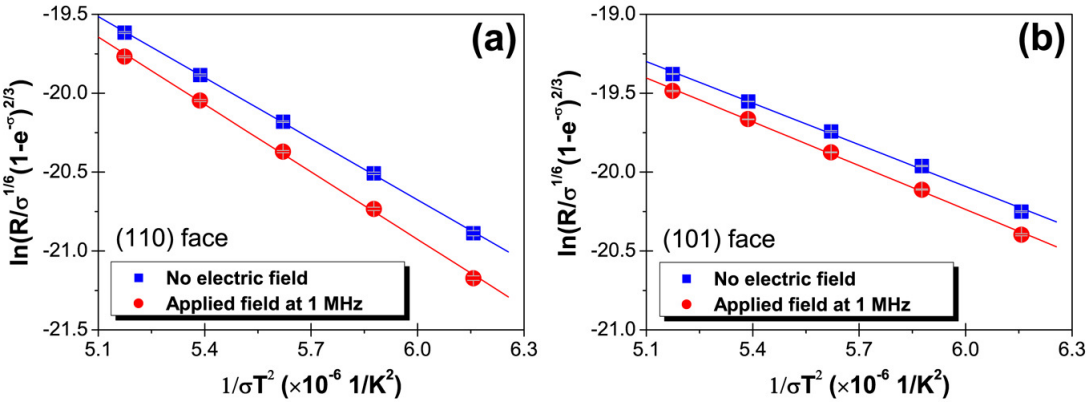

Figure 4. Growth rate R with and without external electric field as function of $1/(\sigma T^2)$. (**a**) (110) face and (**b**) (101) face.

For both faces, α is seen to be approximately 5% larger in the presence of the electric field. This would makes steps more difficult to form, thus leading to a flatter crystal surface. This could also prevent impurities from being incorporated into the steps during crystal growth, which would result in a decrease in the misorientation between subgrains. Therefore, the improved crystal quality for tetragonal HEW lysozyme crystals under a 1 MHz applied field may be predominantly caused by the increase in the effective surface energy of the step ends.

4. Discussion

Let us thermodynamically consider the increase in the effective surface energy of the step ends under an applied field. During nucleation, electrostatic energy is added to the chemical potentials of the liquid and solid phases by the electric field, which leads to an increase in the driving force for nucleation [50]. This would seem to suggest that the growth velocity would also increase. However, in the present study, the electric field was found to cause a reduction in the growth rate. Thus, the increase in the effective surface energy of step ends due to the electrostatic energy may overcome the increase in the driving force for nucleation. Employing the Helmholtz free energy, the free energy on the crystal surface F_s can be expressed as:

$$F_s = U_s - TS_s, \tag{8}$$

where U_s is the energy required for formation of a step and S_s is the entropy related to the shape of the step. Therefore, the electrostatic energy added to the energy required for step formation and the entropy related to the shape of the step must be considered. The modified energy due to formation of the step $U_{s(E)}$, and the modified entropy related to a shape of the step $S_{s(E)}$, can be derived from the Helmholtz free energy:

$$U_{s(E)} = U_{s(0)} + \frac{1}{2}V_c E^2[\epsilon - T\frac{\partial \epsilon}{\partial T}], \tag{9}$$

$$S_{s(E)} = S_{s(0)} - \frac{1}{2}V_c E^2 \frac{\partial \epsilon}{\partial T}, \tag{10}$$

where $U_{s(0)}$ and $S_{s(0)}$ are the energy required for formation of the step and the entropy related to the shape of the step without an external electric field, respectively, T is the absolute temperature, ϵ is the electrical permittivity, E is the strength of the external electric field, and V_c is the volume to which the external electric field is applied. Therefore, the free energy on the crystal surface would

increase if the energy required to form the step increases or the entropy related to the shape of the step decreases under an external electric field.

First, let us consider the effect of the external electric field on the entropy. The dependence of the electrical permittivity of protein crystals on the temperature has been measured using monoclinic lysozyme crystals [71], whereby the sign of the derivative for protein crystals is positive (i.e., the entropy related to the shape of the step decreases under an external electric field). On the other hand, whether the energy required to form the step increases or decreases is attributed to the magnitude between the electrical permittivity and the temperature dependence of the electrical permittivity, as seen in Equation (9). The temperature dependence of the electrical permittivity for protein crystals can be estimated to be about 10^{-11} C^2/Nm^2K using the data reported by Rashkovich et al. [71], whereas the electrical permittivity for protein crystals has been measured to be about 10^{-10} C^2/Nm^2 [71]. Thus, $\epsilon - T\frac{\partial \epsilon}{\partial T}$ is negative, which leads to a reduction of the energy required to form a step under an external electric field. Thus, under an applied field, the increase in the effective surface energy of the step end could be caused by a decrease in the entropy related to the shape of the step. That is, the improvement in crystal quality under an electric field could be due to a decrease in the entropy related to the shape of the step.

In addition, this result could indicate that control of the effective surface energy of the step ends would play an important role in the growth of high-quality protein crystals, which could be achieved by a decrease in the entropy related to the shape of steps and/or an increase in the energy required to form steps.

Acknowledgments: This work was supported in part by a Grant-in-Aid for Challenging Exploratory Research (No. 15K14484) from the Ministry of Education, Culture, Sports, Science and Technology of Japan.

Author Contributions: The study was designed by Haruhiko Koizumi; The experimental results were discussed by all authors.

Conflicts of Interest: The authors declare no conflicts of interests.

References

1. Kuhn, P.; Wilson, K.; Patch, M.G.; Stevens, R.C. The genesis of high-throughput structure-based drug discovery using protein crystallography. *Curr. Opin. Chem. Biol.* **2002**, *6*, 704–710.
2. Chayen, N.E.; Helliwell, J.R.; Snell, E.H. *Macromolecular Crystallization and Crystal Perfection*; Oxford University Press: Oxford, UK, 2010.
3. Sato, T.; Yamada, Y.; Saijo, S.; Hori, T.; Hirose, R.; Tanaka, N.; Sazaki, G.; Nakajima, K.; Igarashi, N.; Tanaka, M.; et al. Enhancement in the perfection of orthorhombic lysozyme crystals grown in a high magnetic field (10 T). *Acta Crystallogr.* **2000**, *D56*, 1079–1083.
4. Lin, S.; Zhou, M.; Azzi, A.; Xu, G.; Wakayama, N.; Ataka, M. Magnet used for protein crystallization: Novel attempts to improve the crystal quality. *Biochem. Biophys. Res. Commun.* **2000**, *275*, 274–278.
5. Ataka, M.; Wakayama, N. Effects of a magnetic field and magnetization force on protein crystal growth. Why does a magnet improve the quality of some crystals? *Acta Crystallogr.* **2002**, *D58*, 1708–1710.
6. Wakayama, N. Effects of a strong magnetic field on protein crystal growth. *Cryst. Growth Des.* **2003**, *3*, 17–24.
7. Kinoshita, T.; Ataka, M.; Warizaya, M.; Neya, M.; Fujii, T. Improving quality and harvest period of protein crystals for structure-based drug design: effects of a gel and a magnetic field on bovine adenosine deaminase crystals. *Acta Crystallogr.* **2003**, *D59*, 1333–1335.
8. Lübbert, D.; Meents, A.; Weckert, E. Accurate rocking-curve measurements on protein crystals grown in a homogeneous magnetic field of 2.4 T. *Acta Crystallogr.* **2004**, *D60*, 987–998.
9. Moreno, A.; Quiroz-García, B.; Yokaichiya, F.; Stojanoff, V.; Rudolph, P. Protein crystal growth in gels and stationary magnetic fields. *Cryst. Res. Technol.* **2007**, *42*, 231–236.
10. DeLucas, L.; Smith, C.; Smith, H.; Vijay-Kumar, S.; Senadhi, S.; Ealick, S.; Carter, D.; Snyder, R.; Weber, P.; Salemme, F. Protein crystal growth in microgravity. *Science* **1989**, *246*, 651–654.
11. McPherson, A. Virus and protein crystal growth on earth and in microgravity. *J. Phys. D* **1993**, *26*, 104–112.

12. Snell, E.; Weisgerber, S.; Helliwell, J.; Weckert, E.; Holzer, K.; Schroer, K. Improvements in lysozyme protein crystal perfection through microgravity growth. *Acta Crystallogr.* **1995**, *D51*, 1099–1102.
13. Sato, M.; Tanaka, H.; Inaka, K.; Shinozaki, S.; Yamanaka, A.; Takahashi, S.; Yamanaka, M.; Hirota, E.; Sugiyama, S.; Kato, M.; et al. JAXA-GCF project-high-quality protein crystals grown under microgravity environment for better understanding of protein structure. *Microgravity Sci. Technol.* **2006**, *18*, 184–189.
14. Takahashi, S.; Tsurumura, T.; Aritake, K.; Furubayashi, N.; Sato, M.; Yamanaka, M.; Hirota, E.; Sano, S.; Kobayashi, T.; Tanaka, T.; et al. High-quality crystals of human haematopoietic prostaglandin D synthase with novel inhibitors. *Acta Crystallogr.* **2010**, *F66*, 846–850.
15. Inaka, K.; Takahashi, S.; Aritake, K.; Tsurumura, T.; Furubayashi, N.; Yan, B.; Hirota, E.; Sano, S.; Sato, M.; Kobayashi, T.; et al. High-quality protein crystal growth of mouse lipocalin-type prostaglandin D synthase in microgravity. *Cryst. Growth Des.* **2011**, *11*, 2107–2111.
16. Yoshikawa, S.; Kukimoto-Niino, M.; Parker, L.; Handa, N.; Terada, T.; Fujimoto, T.; Terazawa, Y.; Wakiyama, M.; Sato, M.; Sano, S.; et al. Structural basis for the altered drug sensitivities of non-small cell lung cancer-associated mutants of human epidermal growth factor receptor. *Oncogene* **2012**, *32*, 27–38.
17. Vekilov, P.G.; Thomas, B.R.; Rosenberger, F. Effects of convective solute and impurity transport in protein crystal growth. *J. Phys. Chem. B* **1998**, *102*, 5208–5216.
18. Kadowaki, A.; Yoshizaki, I.; Adachi, S.; Komatsu, H.; Odawara, O.; Yoda, S. Effects of forced solution flow on protein-crystal quality and growth process. *Cryst. Growth Des.* **2006**, *6*, 2398–2403.
19. Otálora, F.; Gavira, J.A.; Ng, J.D.; García-Ruiz, J.M. Counterdiffusion methods applied to protein crystallization. *Prog. Biophys. Mol. Biol.* **2009**, *101*, 26–37.
20. Maruyama, M.; Kawahara, H.; Sazaki, G.; Maki, S.; Takahashi, Y.; Yoshikawa, H.Y.; Sugiyama, S.; Adachi, H.; Takano, K.; Matsumura, H.; et al. Effects of a forced solution flow on the step advancement on {110} faces of tetragonal lysozyme crystals: direct visualization of individual steps under a forced solution flow. *Cryst. Growth Des.* **2012**, *12*, 2856–2863.
21. Garcia-Ruiz, J.; Moreno, A. Investigations on protein crystal growth by the gel acupuncture method. *Acta Crystallogr.* **1994**, *D50*, 484–490.
22. Vidal, O.; Robert, M.; Arnoux, B.; Capelle, B. Crystalline quality of lysozyme crystals grown in agarose and silica gels studied by X-ray diffraction techniques. *J. Cryst. Growth* **1999**, *196*, 559–571.
23. Lorber, B.; Sauter, C.; Ng, J.; Zhu, D.; Giegé, R.; Vidal, O.; Robert, M.; Capelle, B. Characterization of protein and virus crystals by quasi-planar wave X-ray topography: A comparison between crystals grown in solution and in agarose gel. *J. Cryst. Growth* **1999**, *204*, 357–368.
24. Dong, J.; Boggon, T.J.; Chayen, N.E.; Raftery, J.; Bi, R.C.; Helliwell, J.R. Bound-solvent structures for microgravity-, ground control-, gel-and microbatch-grown hen egg-white lysozyme crystals at 1.8 A resolution. *Acta Crystallogr.* **1999**, *D55*, 745–752.
25. Garcıa-Ruiz, J.; Novella, M.; Moreno, R.; Gavira, J. Agarose as crystallization media for proteins: I: Transport processes. *J. Cryst. Growth* **2001**, *232*, 165–172.
26. Gavira, J.A.; García-Ruiz, J.M. Agarose as crystallisation media for proteins II: Trapping of gel fibres into the crystals. *Acta Crystallogr.* **2002**, *D58*, 1653–1656.
27. Sugiyama, S.; Maruyama, M.; Sazaki, G.; Hirose, M.; Adachi, H.; Takano, K.; Murakami, S.; Inoue, T.; Mori, Y.; Matsumura, H. Growth of protein crystals in hydrogels prevents osmotic shock. *JACS* **2012**, *134*, 5786–5789.
28. Maruyama, M.; Hayashi, Y.; Yoshikawa, H.Y.; Okada, S.; Koizumi, H.; Tachibana, M.; Sugiyama, S.; Adachi, H.; Matsumura, H.; Inoue, T.; et al. A crystallization technique for obtaining large protein crystals with increased mechanical stability using agarose gel combined with a stirring technique. *J. Cryst. Growth* **2016**, *452*, 172–178.
29. Sleutel, M.; Sazaki, G.; Van Driessche, A.E. Spiral-mediated growth can lead to crystals of higher purity. *Cryst. Growth Des.* **2012**, *12*, 2367–2374.
30. Sleutel, M.; Van Driessche, A.E. On the self-purification cascade during crystal growth from solution. *Cryst. Growth Des.* **2013**, *13*, 688–695.
31. Hayashi, Y.; Maruyama, M.; Yoshimura, M.; Okada, S.; Yoshikawa, H.Y.; Sugiyama, S.; Adachi, H.; Matsumura, H.; Inoue, T.; Takano, K.; et al. Spiral growth can enhance both the normal growth rate and quality of tetragonal lysozyme crystals grown under a forced solution flow. *Cryst. Growth Des.* **2015**, *15*, 2137–2143.

32. Tominaga, Y.; Maruyama, M.; Yoshimura, M.; Koizumi, H.; Tachibana, M.; Sugiyama, S.; Adachi, H.; Tsukamoto, K.; Matsumura, H.; Takano, K.; et al. Promotion of protein crystal growth by actively switching crystal growth mode via femtosecond laser ablation. *Nat. Photonics* **2016**, *10*, 723–726.
33. Taleb, M.; Didierjean, C.; Jelsch, C.; Mangeot, J.; Capelle, B.; Aubry, A. Crystallization of proteins under an external electric field. *J. Cryst. Growth* **1999**, *200*, 575–582.
34. Taleb, M.; Didierjean, C.; Jelsch, C.; Mangeot, J.; Aubry, A. Equilibrium kinetics of lysozyme crystallization under an external electric field. *J. Cryst. Growth* **2001**, *232*, 250–255.
35. Nanev, C.; Penkova, A. Nucleation of lysozyme crystals under external electric and ultrasonic fields. *J. Cryst. Growth* **2001**, *232*, 285–293.
36. Charron, C.; Didierjean, C.; Mangeot, J.; Aubry, A. TheOctopus' plate for protein crystallization under an electric field. *J. Appl. Crystallogr.* **2003**, *36*, 1482–1483.
37. Mirkin, N.; Frontana-Uribe, B.; Rodríguez-Romero, A.; Hernández-Santoyo, A.; Moreno, A. The influence of an internal electric field upon protein crystallization using the gel-acupuncture method. *Acta Crystallogr.* **2003**, *D59*, 1533–1538.
38. Moreno, A.; Sazaki, G. The use of a new ad hoc growth cell with parallel electrodes for the nucleation control of lysozyme. *J. Cryst. Growth* **2004**, *264*, 438–444.
39. Penkova, A.; Gliko, O.; Dimitrov, I.; Hodjaoglu, F.; Nanev, C.; Vekilov, P. Enhancement and suppression of protein crystal nucleation due to electrically driven convection. *J. Cryst. Growth* **2005**, *275*, 1527–1532.
40. Penkova, A.; Pan, W.; Hodjaoglu, F.; Vekilov, P. Nucleation of protein crystals under the influence of solution shear flow. *Ann. N. Y. Acad. Sci.* **2006**, *1077*, 214–231.
41. Al-Haq, M.; Lebrasseur, E.; Choi, W.; Tsuchiya, H.; Torii, T.; Yamazaki, H.; Shinohara, E. An apparatus for electric-field-induced protein crystallization. *J. Appl. Crystallogr.* **2007**, *40*, 199–201.
42. Al-Haq, M.; Lebrasseur, E.; Tsuchiya, H.; Torii, T. Protein crystallization under an electric field. *Crystallogr. Rev.* **2007**, *13*, 29–64.
43. Hammadi, Z.; Astier, J.; Morin, R.; Veesler, S. Protein crystallization induced by a localized voltage. *Cryst. Growth Des.* **2007**, *7*, 1472–1475.
44. Pérez, Y.; Eid, D.; Acosta, F.; Marín-García, L.; Jakoncic, J.; Stojanoff, V.; Frontana-Uribe, B.; Moreno, A. Electrochemically assisted protein crystallization of commercial cytochrome c without previous purification. *Cryst. Growth Des.* **2008**, *8*, 2493–2496.
45. Mirkin, N.; Jaconcic, J.; Stojanoff, V.; Moreno, A. High resolution X-ray crystallographic structure of bovine heart cytochrome c and its application to the design of an electron transfer biosensor. *Proteins Struct. Funct. Bioinf.* **2008**, *70*, 83–92.
46. Hou, D.; Chang, H. ac field enhanced protein crystallization. *Appl. Phys. Lett.* **2008**, *92*, 223902.
47. Revalor, E.; Hammadi, Z.; Astier, J.; Grossier, R.; Garcia, E.; Hoff, C.; Furuta, K.; Okustu, T.; Morin, R.; Veesler, S. Usual and unusual crystallization from solution. *J. Cryst. Growth* **2010**, *312*, 939–946.
48. Wakamatsu, T. Transparent cell for protein crystallization under low applied voltage. *Jpn. J. Appl. Phys.* **2011**, *50*, 048003.
49. Wakamatsu, T.; Toyoshima, S.; Shimizu, H. Observation of electric-field induced aggregation in crystallizing protein solutions by forward light scattering. *Appl. Phys. Lett.* **2011**, *99*, 153701.
50. Koizumi, H.; Fujiwara, K.; Uda, S. Control of nucleation rate for tetragonal hen-egg white lysozyme crystals by application of an electric field with variable frequencies. *Cryst. Growth Des.* **2009**, *9*, 2420–2424.
51. Koizumi, H.; Tomita, Y.; Uda, S.; Fujiwara, K.; Nozawa, J. Nucleation rate enhancement of porcine insulin by application of an external AC electric field. *J. Cryst. Growth* **2012**, *352*, 155–157.
52. Koizumi, H.; Fujiwara, K.; Uda, S. Role of the electric double layer in controlling the nucleation rate for tetragonal hen egg white lysozyme crystals by application of an external electric field. *Cryst. Growth Des.* **2010**, *10*, 2591–2595.
53. Koizumi, H.; Uda, S.; Fujiwara, K.; Tachibana, M.; Kojima, K.; Nozawa, J. Improvement of crystal quality for tetragonal hen-egg white lysozyme crystals under application of an external AC electric field. *J. Appl. Crystallogr.* **2013**, *46*, 25–29.
54. Koizumi, H.; Uda, S.; Fujiwara, K.; Tachibana, M.; Kojima, K.; Nozawa, J. Enhancement of crystal homogeneity of protein crystals under application of an external alternating current electric field. *AIP Conf. Proc.* **2014**, *1618*, 265–268.

55. Koizumi, H.; Uda, S.; Fujiwara, K.; Tachibana, M.; Kojima, K.; Nozawa, J. Control of subgrain formation in protein crystals by the application of an external electric field. *Cryst. Growth Des.* **2014**, *14*, 5662–5667.
56. Iimura, Y.; Yoshizaki, I.; Rong, L.; Adachi, S.; Yoda, S.; Komatsu, H. Development of a reusable protein seed crystal processed by chemical cross-linking. *J. Cryst. Growth* **2005**, *275*, 554–560.
57. Koizumi, H.; Tachibana, M.; Yoshizaki, I.; Fukuyama, S.; Tsukamoto, K.; Suzuki, Y.; Uda, S.; Kojima, K. Dislocations in high-quality glucose isomerase crystals grown from seed crystals. *Cryst. Growth Des.* **2014**, *14*, 5111–5116.
58. Koizumi, H.; Uda, S.; Tachibana, M.; Tsukamoto, K.; Kojima, K.; Nozawa, J. Crystallization technique for strain-free protein crystals using cross-linked seed crystals. *Cryst. Growth Des.* **2016**, *16*, 6089–6094.
59. Cacioppo, E.; Pusey, M.L. The solubility of the tetragonal form of hen egg white lysozyme from pH 4.0 to 5.4. *J. Cryst. Growth* **1991**, *114*, 286–292.
60. Huang, X.; Uda, S.; Yao, X.; Koh, S. In situ observation of crystal growth process of YBCO superconductive oxide with an external electric field. *J. Cryst. Growth* **2006**, *294*, 420–426.
61. Huang, X.; Uda, S.; Koh, S. Effect of an external electric field on the crystal growth process of YBCO superconductive oxide. *J. Cryst. Growth* **2007**, *307*, 432–439.
62. Van Driessche, A.E.; Sazaki, G.; Otálora, F.; González-Rico, F.M.; Dold, P.; Tsukamoto, K.; Nakajima, K. Direct and noninvasive observation of two-dimensional nucleation behavior of protein crystals by advanced optical microscopy. *Cryst. Growth Des.* **2007**, *7*, 1980–1987.
63. Malkin, A.; Chernov, A.; Alexeev, I. Growth of dipyramidal face of dislocation-free ADP crystals; free energy of steps. *J. Cryst. Growth* **1989**, *97*, 765–769.
64. Sleutel, M.; Willaert, R.; Gillespie, C.; Evrard, C.; Wyns, L.; Maes, D. Kinetics and thermodynamics of glucose isomerase crystallization. *Cryst. Growth Des.* **2008**, *9*, 497–504.
65. Vekilov, P.G.; Alexander, J.I.D. Dynamics of layer growth in protein crystallization. *Chem. Rev.* **2000**, *100*, 2061–2090.
66. Durbin, S.; Feher, G. Studies of crystal growth mechanisms of proteins by electron microscopy. *J. Mol. Biol.* **1990**, *212*, 763–774.
67. Durbin, S.D.; Carlson, W.E. Lysozyme crystal growth studied by atomic force microscopy. *J. Cryst. Growth* **1992**, *122*, 71–79.
68. Konnert, J.H.; D'Antonio, P.; Ward, K. Observation of growth steps, spiral dislocations and molecular packing on the surface of lysozyme crystals with the atomic force microscope. *Acta Crystallogr.* **1994**, *D50*, 603–613.
69. Li, H.; Nadarajah, A.; Pusey, M.L. Determining the molecular-growth mechanisms of protein crystal faces by atomic force microscopy. *Acta Crystallogr.* **1999**, *D55*, 1036–1045.
70. Markov, I.V. *Crystal Growth for Beginners: Fundamentals of Nucleation, Crystal Growth and Epitaxy*; World Scientific: Singapore, 2003.
71. Rashkovich, L.; Smirnov, V.; Petrova, E. Some dielectric properties of monoclinic lysozyme crystals. *Phys. Solid State* **2008**, *50*, 631–637.